Journal of Quantitative Spectroscopy & Radiative Transfer 210 (2018) 165–172

Contents lists available at ScienceDirect

Journal of Quantitative Spectroscopy & Radiative Transfer

journal homepage: www.elsevier.com/locate/jqsrt

Synchronous scattering and diffraction from gold nanotextured surfaces with structure factors

Min-Jhong Gu[a], Ming-Tsang Lee[b], Chien-Hsun Huang[a], Chi-Chun Wu[a], Yu-Bin Chen[a,c,*]

[a] Department of Mechanical Engineering, National Cheng Kung University, No. 1, University Road, Tainan City 70101, Taiwan
[b] Department of Mechanical Engineering, National Chung Hsing University, No. 145, Xingda Rd., South Dist., Taichung City 402, Taiwan
[c] Department of Power Mechanical Engineering, National Tsing Hua University, No.101, Kuang Fu Road, Hsinchu City 30013, Taiwan

ARTICLE INFO

Article history:
Received 19 October 2017
Revised 22 January 2018
Accepted 5 February 2018
Available online 7 February 2018

Keywords:
Diffraction
Periodic structures
Roughness
Scattering

ABSTRACT

Synchronous scattering and diffraction were demonstrated using reflectance from gold nanotextured surfaces at oblique ($\theta_i = 15°$ and 60°) incidence of wavelength $\lambda = 405$ nm. Two samples of unique auto-correlation functions were cost-effectively fabricated. Multiple structure factors of their profiles were confirmed with Fourier expansions. Bi-directional reflectance function (BRDF) from these samples provided experimental proofs. On the other hand, standard deviation of height and unique auto-correlation function of each sample were used to generate surfaces numerically. Comparing their BRDF with those of totally random rough surfaces further suggested that structure factors in profile could reduce specular reflection more than totally random roughness.

1. Introduction

Optical responses of non-smooth surfaces have fertilized various applications. For instance, enhanced light absorption benefits throughput of opto-electronic devices [1-4]. Spatial intensity distribution of reflected electromagnetic waves can be interpreted to identify surface profiles [5-8]. Other applications include spectral modulation of absorption/emission [9, 10], enlargement of Raman scattering [11, 12], excitation of diversified resonances [13, 14], and frequency shift or magnification of a resonance [15, 16]. Among these applications, the non-smooth surfaces were totally random rough or periodically structured. The former surfaces have a height histogram following normal distribution, and their auto-correlation functions (ACF) obey the Gaussian [17] or exponential [7, 18, 19] function. Correlation between heights at two locations monotonically reduces with distance between the two locations. In contrast to totally random rough surfaces, the profile of periodically structured surfaces repeats itself precisely every period Λ. The height variation within a period may be significant such that its histogram does not follow normal distribution. ACF of these surfaces is periodic, and the period is identical to that of surface profile.

The profile of slightly periodic surfaces is neither totally random rough nor periodically structured. These surfaces have been found on glass after being processed by laser [20] and dielectrics after physically grinding [21]. Their height histogram follows normal distribution, while their ACF's exhibit oscillations. Heights at positions far apart are sometimes positively correlated like those of a periodic surface. But other times heights are negatively correlated or uncorrelated like those of a totally random rough surface. These surfaces of oscillating ACF's are thus considered slightly periodic or profiles having multiple structure factors. However, their optical responses were rarely investigated and compared with those from counterparts, such as totally random rough and exactly periodic surfaces. As a result, this work is going to study their bi-directional reflectance distribution function (BRDF), the most fundamental response, from non-absorbing metallic surfaces at different angle of incidence.

Both experimental and numerical investigations were conducted, and their results will be presented. Preparation of samples will be briefed, and their profile characteristics will be specified. Their ACF and standard deviation of height (σ) will be used to confirm the success of surface generation as well as to identify dominant structure factors. Next, the measured σ and ACF will be adopted to numerically generate slightly rough surfaces in modeling. Totally random rough surfaces having the same σ and their ACF following Gaussian statistics will be also generated. The former and later surfaces are symbolized with *Model* and *Gauss* hereafter,

Abbreviations: ACF, auto-correlation function; BRDF, bi-directional reflectance distribution function; FDTD, finite difference time domain; TE, transverse electric; TM, transverse magnetic.

* Corresponding author at: Department of Power Mechanical Engineering, National Tsing Hua University, No.101, Kuang Fu Road, Hsinchu City 30013, Taiwan.
E-mail address: ybchen@pme.nthu.edu.tw (Y.-B. Chen).

https://doi.org/10.1016/j.jqsrt.2018.02.007
0022-4073/

Nomenclature

C	coefficient of Fourier series, m
F	reconstructed surface profile
h	height, m
I	spectral intensity, W/m^2/μm/sr
m	diffraction order
n	refractive index
x, y, z	Cartesian coordinate system
Greek symbols	
δ	penetration depth, m
θ	polar angle, degree
κ	extinction coefficient
Λ	period and structure factor, m
λ	wavelength, m
ρ''_λ	spectral bi-directional reflectance distribution function
σ	standard deviation of height, m
τ	distance, m
φ	azimuthal angle, degree
ω	solid angle, sr
Subscripts	
A, B	surface A, B
d	dominant terms in Fourier series
i	incidence
r	reflectance
$\bar{x}, \bar{y}$	average along the x- and y-direction
6	6-μm-long period

respectively. Reflectance from these numerically generated surfaces will be acquired to compare with that measured from real samples. Uniqueness in reflectance caused by structure factors will be exhibited and discussed.

2. Sample preparation and surface analysis

Fabricating of a sample was composed of roughening a silicon piece and coating it with metallic films. Roughness on the silicon piece was scratched using a home-built grinder [21]. The grinder was composed of a Scotch yoke, Roberval balance, and driving motor. The Scotch yoke turned rotary motion of the driving motor into linearly back-and-forth motion of a platform. Bottom of the platform was attached to a piece of sandpaper. The linear motion of sandpaper was then able to scratch surfaces only along such direction. The Roberval balance had another two platforms. The upper platform supported a silicon piece with its top surface being scratched, while the lower platform held a weight. A constant weight (2 kg) was loaded to give uniform pressure between the sample and sandpaper throughout the fabrication.

Each silicon piece was 40×40 mm^2, diced from a 508-μm-thick and double-side polished crystalline wafer. The crystal orientation (100) was set parallel to the linear motion of platform on Scotch yoke during 50-minute-long scratching. Sandpapers were renewed regularly to assure roughness uniformity. Two types of sandpaper were employed, and average diameters of their SiC sands were 35 μm and 15 μm. After scratching, silicon pieces were cleaned using de-ionized water and purged with nitrogen. Pieces scratched by larger and smaller sands became supporting substrates of A-type and B-type surfaces, respectively.

Profile of silicon pieces was measured using a contact mode of an AFM (Veeco D5000) with a tip of 7-nm-radius. The AFM stage resolution along lateral and vertical directions was 1.5 nm and 0.1 nm, respectively. Total 3 sampling areas were scanned for each piece. A scanning area was 10 μm × 10 μm, and 512 × 512 data points of height $h(x, y)$ were recorded. $h_{\bar{x},\bar{y}}$ was the average of height, where the subscript $\bar{x}, \bar{y}$ symbolize the average over both x- and y-directions within the piece. The height standard deviation ($\sigma_{\bar{x},\bar{y}}$) could be obtained in the following:

$$\sigma_{\bar{x},\bar{y}} = \sqrt{\frac{\left[h(x,y) - h_{\bar{x},\bar{y}}\right]^2}{3 \cdot 512 \cdot 512 - 1}} \tag{1}$$

The $\sigma_{\bar{x},\bar{y}}$ were 58 nm and 35 nm for A-type and B-type surfaces, respectively. That is, larger sand particles brought about a rougher profile, i.e., larger $\sigma_{\bar{x},\bar{y}}$.

Each roughened silicon piece was then coated with metallic films exploiting a physical vapor deposition technique [22]. During deposition, target metal billets in a crucible were heated into vapor. The crucible was under a silicon piece and faced directly to the roughened surface. Evaporated metallic atoms from the crucible were condensed and solidified on the rough surface slowly. The silicon surface was then gradually covered by a film. Thickness of the film could be controlled by deposition time. A 10-nm-thick Cr layer was deposited as an adhesive layer before coating a 100-nm-thick Au film. After coating two metals, A-type and B-type surfaces became Sample A and Sample B, respectively. Their profiles were measured using the above-mentioned AFM again. The $\sigma_{\bar{x},\bar{y}}$ averaged over 3 areas of Sample A and Sample B were 57 nm and 47 nm, respectively. It is clear that a rougher silicon substrate led to a rougher Au surface, i.e., $\sigma_{\bar{x},\bar{y}}$ is lager for Sample A than Sample B. Because $\sigma_{\bar{x},\bar{y}}$ did not vary much before and after coating, many profile characteristics were transferred from silicon to Au. Reasons for imperfect profile transfer were non-uniform film thickness and inconsistent sampling areas. Although two metallic films were on a sample, Sample A and Sample B could be viewed as rough surfaces above a semi-infinite Au substrate because the 100-nm-thick Au was opaque to 405-nm-wavelength light studied here. Au was selected for its resistance to oxidation, popularity in diversified applications, and capability in exciting surface plasmon [23].

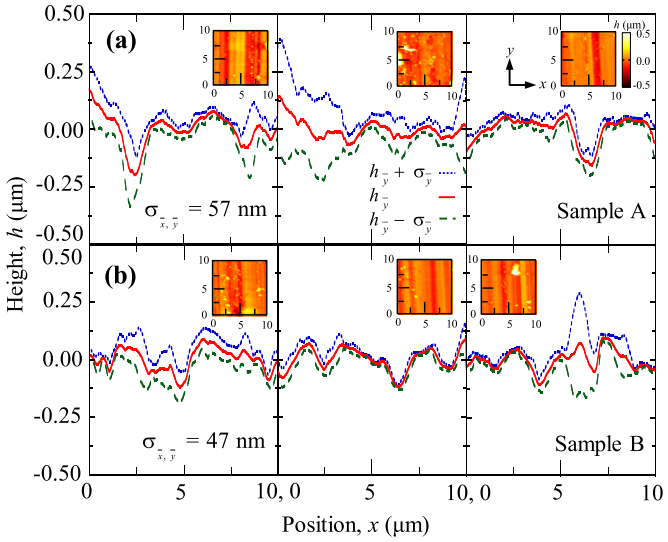

Fig. 1. Cross-sectional view of sample height averaged along y-direction $h_{\bar{y}}$ and its two bounds $h_{\bar{y}} \pm \sigma_{\bar{y}}$ for: (a) Sample A; (b) Sample B. The inset is contour of measured height before averaging.

Fig. 1(a) and (b) show measured height $h(x, y)$ of 3 areas from Sample A and B, respectively. Because samples were scratched along the y-direction during fabrication, surface profiles varied insignificantly along that direction. In contrast, the profile varied much along the x-direction. For a fixed x, $h_{\bar{y}}(x)$ was the height av-